AN UPSCALING METHOD FOR ONE-PHASE FLOW IN HETEROGENEOUS RESERVOIRS; A WEIGHTED OUTPUT LEAST SQUARES (WOLS) APPROACH

BJØRN FREDRIK NIELSEN* AND ASLAK TVEITO**

Abstract. In this paper we study the problem of determining the effective permeability on a coarse scale level of problems with strongly varying and discontinuous coefficients defined on a fine scale. The upscaled permeability is defined as the solution of an optimization problem, where the difference between the fine scale and the coarse scale velocity field is minimized. We show that it is not necessary to solve the fine scale pressure equation in order to minimize the associated cost-functional. Furthermore, we derive a simple technique for computing the derivatives of the cost-functional needed in the fix-point iteration used to compute the optimal permeability on the coarse mesh. Finally, the method is illustrated by several analytical examples and numerical experiments.

Key words. reservoir simulation, second order elliptic equations, upscaling, homogenization.

AMS subject classifications. 35J25, 35J20, 73B27.

1. Introduction. The data describing the basic geophysical properties of a reservoir are important input to any method for simulating the production of hydrocarbons. These data, usually generated by geostatistical methods, are often given on a very fine scale. This fine scale model cannot be used directly in a reservoir simulator as the associated degrees of freedom is out of scope for todays computers. Thus the data have to be upscaled to a coarser representation before they are used in a simulator, cf. [6, 9, 11, 12, 17, 18, 19, 21, 29].

The purpose of the present paper is to introduce a new technique for assigning permeabilities to a coarse mesh based on a fine mesh representation. Our approach is to minimize, in proper norms, the error introduced in the velocity field by the upscaling process. More precisely, we suggest a scheme for computing the best upscaled permeability field in the sense that the difference between the fine scale velocity and the coarse scale velocity is minimized. This approach is reasonable since the velocity field is the main input to the flow simulator. The main technical feature of our ap-

*The Norwegian Computing Center, P.O. Box 114 Blindern, N-0314 Oslo, Norway. Email: Bjorn.Fredrik.Nielsen@nr.no. This author's work has been supported by The Research Council of Norway (NFR) under grant no. 107643/431 and the Norwegian Computing Center. Part of this author's work was done at the Institut für Mathematik, Johannes-Kepler-Universität, Linz, Austria.

**Department of Informatics, University of Oslo, P.O. Box 1080 Blindern, N-0316 Oslo, Norway. Email: aslak@ifi.uio.no. This author's work has been supported The Research Council of Norway (NFR) under grant no. 110673/420 (Numerical Computations in Applied Mathematics).

proach is that we avoid solving the pressure equation on the fine scale. Our technique is developed for one-phase flow in heterogeneous reservoirs. However, it should be mentioned that the technique also is applicable to multi-phase problems and that this sort of problem arise in a series of mechanical, chemical and several other engineering problems.

The problem of computing the permeability values for the coarse scale grid-blocks has been of interest for many years. The simplest methods are defined in terms of some average of the fine scale data. Typically, the coarse scale permeabilities are computed as the arithmetic, geometric or harmonic mean of the fine scale permeabilities, cf. e.g. Dale, Ekrann and Holden [25], Deutsch [9] or references given therein. These methods are computationally efficient, but inaccurate for problems with strong permeability variations.

A more accurate, though computationally more expensive, method is based on solving the flow equation on each coarse grid-block. A no flow boundary condition is applied to all faces of the block except for two opposite faces where constant Dirichlet boundary conditions are applied. The coarse grid-block permeability is then determined such that the total flow across the block is preserved, see Durlefski [12], Warren and Price [29] and Desbarats [11].

Furthermore, King [21] has suggested a renormalization procedure and Griebel and Knapek [17] use a multigrid technique for upscaling. Under the assumption of periodic structures, homogenization methods can be applied [3, 5, 20]. Further interesting analyses of homogenization problems and their applications can be found in [1, 2, 26, 27], cf. also the references given in these papers. .

The rest of this paper is organized as follows: In the next section we introduce our upscaling technique. Thereafter we show that it is not necessary to solve the fine scale pressure equation in order to compute the coarse scale permeabilities. Section 3 contains some simple analytical examples illustrating important properties of this upscaling technique. In Section 4 we present an algorithm for computing the coarse scale permeabilities. Section 5 contains the numerical experiments, and in Section 6 we state some concluding remarks.

2. Upscaling. For simplicity, we consider a two-dimensional reservoir. The method is generalized to 3D in a straight forward manner.

Let P represent the unknown fluid pressure related to one-phase flow in a heterogeneous reservoir, g the gravitational constant, ρ the density of the fluid and D the depth of the reservoir measured in the direction of gravity. Then the pressure

equation arising in reservoir simulation can be written on the form

$$\nabla \cdot [\Lambda (\nabla P - \rho g \nabla D)] + \frac{q}{\rho} = 0 \quad \text{in } \Omega \subset \mathbb{R}^2, \tag{2.1}$$

see for instance Ewing [15] or Peaceman [24]. This equation results from Darcy's law and conservation of mass. In (2.1), the function Λ describes the permeability of the reservoir and can be a scalar or tensor function. Normally, Λ would be the so-called mobility function representing, not only the permeability of the medium, but also other physical parameters such as the viscosity of the fluid in question. However, in this paper we will always refer to Λ as the absolute permeability. Source terms, such as injection and production wells located inside Ω, are incorporated in the model (2.1) by the function q.

Throughout this paper we will assume that ρ and g are given constants. Then, by putting $f = q/\rho$ and $p = P - \rho g D$ the pressure equation (2.1) can be rewritten on the form

$$\nabla \cdot [\Lambda \nabla p] + f = 0 \quad \text{in } \Omega \subset \mathbb{R}^2. \tag{2.2}$$

Next, we assume that the reservoir is surrounded by non-permeable rocks. Hence, we have a no-flow boundary condition on the entire boundary, i.e.

$$\mathbf{v} \cdot \mathbf{n} = 0 \quad \text{on } \partial\Omega, \tag{2.3}$$

where $\mathbf{n}$ denotes the outwards directed normal vector of unit length, while the Darcy velocity $\mathbf{v}$ is defined as

$$\mathbf{v} = -\Lambda \nabla p. \tag{2.4}$$

Often, the absolute permeability Λ is defined in terms of a fine grid on Ω, i.e. Λ is constant on each fine grid-block. Normally, this representation of Λ is not suitable for reservoir simulators and Λ must be upscaled[1]. This upscaling problem can roughly be formulated as follows: We want to replace Λ in (2.2)-(2.3) by a so-called effective permeability Λ_e, defined in terms of a coarse grid on Ω, such that the resulting velocity field

$$\mathbf{v}_e = -\Lambda_e \nabla p_e$$

is a good approximation of the fine scale velocity field $\mathbf{v}$, defined in (2.4). Here, p_e is the solution of the coarse scale pressure equation

$$\nabla \cdot [\Lambda_e \nabla p_e] + f = 0 \quad \text{in } \Omega \subset \mathbb{R}^2,$$

$$\mathbf{v}_e \cdot \mathbf{n} = 0 \quad \text{on } \partial\Omega.$$

[1] The reason for this is that the data are generated by geostatistical methods; the actual physical data are sparse.

As mentioned above, our approach to this problem is to determine Λ_e such that the difference between the fine scale velocity field $\mathbf{v}$ and the coarse scale velocity $\mathbf{v}_e$ field is minimized. In order to describe the method, we need to introduce some notation and the weak formulation of the boundary value problem (2.2)-(2.3).

Let $\{\Omega_i\}_{i=1}^N$ be a set of coarse grid-blocks satisfying

$$\overline{\Omega} = \bigcup_{i=1}^{N} \overline{\Omega}_i \text{ and } \Omega_i \bigcap \Omega_j = \emptyset \text{ for } i \neq j, \tag{2.5}$$

then we can define the set Q of admissible coarse scale permeabilities as follows

$$\begin{aligned} Q = \{\Lambda_H : \Omega \to \mathbb{R}_+;\ & \Lambda_H|_{\Omega_i} \text{ is constant for } i = 1, \ldots, N, \\ & \text{and } 0 < \Lambda_H(x) < \infty \text{ for all } x \in \Omega\}. \end{aligned} \tag{2.6}$$

We are going to determine Λ_e in Q such that the difference between $\mathbf{v}$ and $\mathbf{v}_e$ is minimized. Notice that if $\Lambda_H \in Q$, then Λ_H is uniformly positive and bounded. In fact, Λ_H is defined by a finite number of positive values. For every $\Lambda_H \in Q$ we define the following boundary value problem

$$\begin{aligned} \nabla \cdot [\Lambda_H \nabla p_H] + f = 0 \quad & \text{in } \Omega \subset \mathbb{R}^2, \\ \mathbf{v}_H \cdot \mathbf{n} = 0 \quad & \text{on } \partial\Omega, \end{aligned} \tag{2.7}$$

and the associated velocity

$$\mathbf{v}_H(\Lambda_H) = -\Lambda_H \nabla p_H(\Lambda_H). \tag{2.8}$$

Let $H^1(\Omega)$ denote the classical Sobolev space of square-integrable functions with square-integrable distributional derivatives. If the subspace $V \subset H^1(\Omega)$ is defined by

$$V = \{\psi \in H^1(\Omega);\ \int_\Omega \psi \, dx = 0\},$$

then the weak formulation of (2.2)-(2.3) can be defined in the usual way: Find $p \in V$ such that

$$\int_\Omega \nabla\psi \cdot (\Lambda \nabla p) \, dx = \int_\Omega f\psi \, dx \quad \text{for all } \psi \in V. \tag{2.9}$$

Next, the weak formulation of (2.7) is: Find $p_H = p_H(\Lambda_H) \in V$ such that

$$\int_\Omega \nabla\psi \cdot (\Lambda_H \nabla p_H(\Lambda_H)) \, dx = \int_\Omega f\psi \, dx \quad \text{for all } \psi \in V. \tag{2.10}$$

In order to get well-posed variational problems (2.9) and (2.10) we must impose some assumptions on f and Λ. More precisely, we assume that $f \in L^2(\Omega)$ satisfying

$$\int_\Omega f \, dx = 0, \tag{2.11}$$

and that the absolute permeability Λ is a uniform positive and bounded function, i.e.

$$0 < m \leq \Lambda(x) \leq M \quad \text{for all } x \in \Omega, \tag{2.12}$$

where m and M are finite constants. In the subspace V of $H^1(\Omega)$ Poincaré's inequality holds, cf. e.g. Dautray and Lions [8]. Hence, if the boundary of Ω is sufficiently smooth, then it follows from (2.11), (2.12) and the Lax-Milgram theorem that the problem (2.9) is well-posed, see e.g. Dautray and Lions [8]. Furthermore, the problem (2.10) has a unique solution $p_H = p_H(\Lambda_H)$ for every $\Lambda_H \in Q$.

2.1. An output least squares formulation of the upscaling problem. We consider a so-called output least squares formulation of the upscaling problem described above. More precisely, we would like to define the effective permeability Λ_e as the solution of an optimization problem of the form

$$\min_{\Lambda_H \in Q} \| \mathbf{v}_H(\Lambda_H) - \mathbf{v} \|^2, \tag{2.13}$$

where $\mathbf{v}_H(\Lambda_H)$ and $\mathbf{v}$ are the velocity fields associated the coarse and fine scale permeability defined as in (2.4) and (2.8), respectively. Here, $\| \cdot \|$ is a suitable norm defined on $L^2(\Omega) \times L^2(\Omega)$. This solution concept, often referred to as an output least squares (OLS) formulation of the problem, is frequently applied to solve inverse problems and parameter identification problems, cf. e.g. Banks and Kunisch [4] and Engl [14]. Clearly, the upscaling problem considered in this paper is a sort parameter identification problem. Thus, we find it appropriate to apply the OLS-formulation. Unfortunately, (2.13) is a nonlinear optimization problem. In addition, parameter identification problems of this type tend to be ill-posed. Therefore, to make sure that we get a well-posed problem and to obtain a simpler minimization problem we apply Tikhonov regularization. That is, the solution of the problem (2.13) is approximated by the solution of the minimization problem

$$\min_{\Lambda_H \in Q} \left(\| \mathbf{v}_H(\Lambda_H) - \mathbf{v} \|^2 + \alpha \| \Lambda_H - \Lambda \|^2_{L^2(\Omega)} \right), \tag{2.14}$$

where $\alpha \geq 0$ is a small positive regularization parameter[2]. Clearly, the regularization term $\alpha \| \Lambda_H - \Lambda \|^2_{L^2(\Omega)}$ is a convex term. Hence, for every $\alpha > 0$ the problem (2.14) is likely to be more well-behaved than the problem (2.13). Furthermore, for small values of α the solution of (2.14) should be a good approximation of the solution of (2.13).

[2]The question whether the problem (2.13) is well-posed or not will not be discussed any further in this paper. For a general treatment of non-linear ill-posed problems we refer to Engl, Kunisch and Neubauer [13].

Obviously, for a general norm $\|\cdot\|$ we have to compute the fine scale velocity field $\mathbf{v}$ in order to solve (2.14). That is, we must solve the fine scale pressure equation (2.9), cf. also (2.4). Obviously, for sufficiently fine scales, that is extremely time-consuming. However, if a special type of norm $\|\cdot\|$ is applied in (2.14), then it turns out that this step can be avoided. Let the $\|\cdot\|_{\Lambda^{-1}}$-norm on $L^2(\Omega) \times L^2(\Omega)$ be defined as follows

$$\|\mathbf{w}\|_{\Lambda^{-1}} = \left(\int_\Omega [\mathbf{w}, \Lambda^{-1}\mathbf{w}]\, dx \right)^{1/2}, \tag{2.15}$$

for $\mathbf{w} \in L^2(\Omega) \times L^2(\Omega)$. Here, $[\cdot,\cdot]$ denotes the Euclidean inner-product on $\mathbb{R}^2$. This is a so-called weighted L^2-norm with weight-function Λ^{-1}. If this norm is applied in (2.14), we obtain the following optimization problem

$$\min_{\Lambda_H \in Q} \left(\|\mathbf{v}_H(\Lambda_H) - \mathbf{v}\|^2_{\Lambda^{-1}} + \alpha \| \Lambda_H - \Lambda \|^2_{L^2(\Omega)} \right). \tag{2.16}$$

In this paper we define the effective permeability Λ_e to be the solution of the problem (2.16). The resulting method for computing the coarse scale permeabilities will be referred to as the Weighted Output Least Squares (WOLS) method. Clearly, to make the error in the velocity field as small as possible we would like to choose α as small as possible. Therefore, whenever possible, we will put α equal to zero.

Let us verify that it is not necessary to solve the fine scale pressure equation (2.9) in order to minimize (2.16). For an arbitrary coarse scale permeability $\Lambda_H \in Q$ we find that

$$\begin{aligned}
\|\mathbf{v}_H(\Lambda_H) - \mathbf{v}\|^2_{\Lambda^{-1}} &= \|\Lambda_H \nabla p_H(\Lambda_H) - \Lambda \nabla p\|^2_{\Lambda^{-1}} \\
&= \int_\Omega [\Lambda_H \nabla p_H(\Lambda_H) - \Lambda \nabla p, \Lambda^{-1}\Lambda_H \nabla p_H(\Lambda_H) - \nabla p]\, dx \\
&= \int_\Omega [\Lambda_H \nabla p_H(\Lambda_H), \Lambda^{-1}\Lambda_H \nabla p_H(\Lambda_H)]\, dx - \int_\Omega [\Lambda_H \nabla p_H(\Lambda_H), \nabla p]\, dx \\
&\quad - \int_\Omega [\Lambda \nabla p, \Lambda^{-1}\Lambda_H \nabla p_H(\Lambda_H)]\, dx + \int_\Omega [\Lambda \nabla p, \nabla p]\, dx. \qquad (2.17)
\end{aligned}$$

Putting $\psi = p \in V$ in (2.10) it follows that

$$\int_\Omega [\Lambda_H \nabla p_H(\Lambda_H), \nabla p]\, dx = \int_\Omega \nabla p \cdot (\Lambda_H \nabla p_H(\Lambda_H))\, dx = \int_\Omega fp\, dx, \tag{2.18}$$

and thus

$$\int_\Omega [\Lambda \nabla p, \Lambda^{-1}\Lambda_H \nabla p_H(\Lambda_H)]\, dx = \int_\Omega \nabla p \cdot (\Lambda_H \nabla p_H(\Lambda_H))\, dx = \int_\Omega fp\, dx. \tag{2.19}$$

Hence, from (2.17)-(2.19) we find that

$$\begin{aligned}
\|\mathbf{v}_H(\Lambda_H) - \mathbf{v}\|^2_{\Lambda^{-1}} = &\int_\Omega [\Lambda_H \nabla p_H(\Lambda_H), \Lambda^{-1}\Lambda_H \nabla p_H(\Lambda_H)]\, dx \\
&-2\int_\Omega fp\, dx + \int_\Omega [\Lambda \nabla p, \nabla p]\, dx
\end{aligned}$$

for every $\Lambda_H \in Q$. Since the two latter terms here are independent of Λ_H, we solve (2.16) by minimizing the following cost-functional

$$J(\Lambda_H) = \int_\Omega [\Lambda_H \nabla p_H(\Lambda_H), \Lambda^{-1} \Lambda_H \nabla p_H(\Lambda_H)]\, dx + \alpha \| \Lambda_H - \Lambda \|^2_{L^2(\Omega)} \tag{2.20}$$

defined on Q. Moreover, it follows that it is not necessary to solve the fine scale pressure equation (2.9).

Remarks.

1. Notice that no particular relation between the fine scale grid and the coarse scale grid is required. In the derivation of the WOLS-method above, no reference to the fine scale grid is made.
2. The permeabilities can be scaler or symmetric and positive definite tensors. However, for the sake of simplicity, we will only consider the scalar case in this paper. In the tensor case, it would probably be more difficult to compute the derivatives of the cost-functional $J(\cdot)$, cf. section 2.2 below.
3. Throughout this paper we will consider two dimensional model problems, i.e. $\Omega \subset \mathbb{R}^2$. However, it should be mentioned that the WOLS-method is also applicable in the case of three space dimensions.

2.2. Differentiation of the cost-functional. Many minimization algorithms require the partial derivatives of the cost-functional. This is, for instance, the case for the method of steepest descent, Newton's method and the conjugate gradient method, cf. e.g. Fletcher [16]. The purpose of this section is to show how the partial derivatives of the cost-functional $J(\cdot)$, defined in (2.20), can be computed efficiently.

Recall that every coarse scale permeability $\Lambda_H \in Q$ is piecewise constant on the coarse grid-blocks $\{\Omega_i\}_{i=1}^N$, cf. (2.6). Therefore, every $\Lambda_H \in Q$ is represented by a finite sequence of positive real numbers $\lambda_1, \ldots, \lambda_N$, such that

$$\Lambda_H(x) = \lambda_i \quad \text{for all } x \in \Omega_i \text{ and } i = 1, \ldots, N.$$

From (2.20) we find that

$$\begin{aligned} J(\Lambda_H) = J(\lambda_1, \ldots, \lambda_N) = & \\ & \sum_{i=1}^N \lambda_i^2 \int_{\Omega_i} [\nabla p_H(\lambda_1, \ldots, \lambda_N), \Lambda^{-1} \nabla p_H(\lambda_1, \ldots, \lambda_N)]\, dx \\ & + \alpha \sum_{i=1}^N \lambda_i^2 |\Omega_i| - 2\alpha \sum_{i=1}^N \lambda_i \int_{\Omega_i} \Lambda \, dx + \alpha \int_\Omega \Lambda^2 \, dx, \end{aligned} \tag{2.21}$$

where $p_H(\lambda_1, \ldots, \lambda_N) = p_H(\Lambda_H)$. Now we want to find a method for computing the partial derivatives $\partial J / \partial \lambda_j$ for $j = 1, \ldots, N$, of the cost-functional $J(\cdot)$. A straight

forward approach to this problem would be to approximate the partial derivatives by finite differences, i.e.

$$\frac{\partial J}{\partial \lambda_j}(\lambda_1, \ldots, \lambda_N) \approx \frac{J(\lambda_1, \ldots, \lambda_j + \Delta\lambda_j, \ldots, \lambda_N) - J(\lambda_1, \ldots, \lambda_j, \ldots, \lambda_N)}{\Delta\lambda_j},$$

for $j = 1, \ldots, N$. Clearly, this approach requires the computation of $p_H(\lambda_1, \ldots, \lambda_j + \Delta\lambda_j, \ldots, \lambda_N)$ for $j = 1, \ldots, N$, cf. (2.21). Hence, $N+1$ coarse scale pressure equations of the form (2.10) must be solved. If the number of coarse scale grid-blocks N is large, then this process would be computationally expensive. However, if an auxiliary problem is introduced, it turns out that it is only necessary to solve two coarse scale problems of the form (2.10) in order to compute all the partial derivatives of $J(\cdot)$, independent of N. In order to see this, we differentiate J with respect to λ_j,

$$\begin{aligned}
\frac{\partial J}{\partial \lambda_j} &= 2\lambda_j \int_{\Omega_j} [\nabla p_H(\lambda_1, \ldots, \lambda_N), \Lambda^{-1} \nabla p_H(\lambda_1, \ldots, \lambda_N)]\, dx \\
&\quad + \sum_{i=1}^{N} \lambda_i^2 \frac{\partial}{\partial \lambda_j} \left[\int_{\Omega_i} [\nabla p_H(\lambda_1, \ldots, \lambda_N), \Lambda^{-1} \nabla p_H(\lambda_1, \ldots, \lambda_N)]\, dx \right] \\
&\quad + 2\alpha\lambda_j |\Omega_j| - 2\alpha \int_{\Omega_j} \Lambda\, dx \\
&= 2\lambda_j \int_{\Omega_j} [\nabla p_H(\lambda_1, \ldots, \lambda_N), \Lambda^{-1} \nabla p_H(\lambda_1, \ldots, \lambda_N)]\, dx \\
&\quad + 2 \sum_{i=1}^{N} \lambda_i^2 \int_{\Omega_i} [\nabla p_H(\lambda_1, \ldots, \lambda_N), \Lambda^{-1} \nabla \left[\frac{\partial p_H}{\partial \lambda_j}(\lambda_1, \ldots, \lambda_N) \right]]\, dx \\
&\quad + 2\alpha\lambda_j |\Omega_j| - 2\alpha \int_{\Omega_j} \Lambda\, dx. \qquad (2.22)
\end{aligned}$$

Thus we have to determine $\partial p_H / \partial \lambda_j$. From equation (2.10) and the definition (2.6) of Q it follows that

$$\sum_{i=1}^{N} \lambda_i \int_{\Omega_i} \nabla\psi \cdot \nabla p_H(\lambda_1, \ldots, \lambda_N)\, dx = \int_{\Omega} f\psi \quad \text{for all } \psi \in V.$$

Again, we differentiate with respect to λ_j to obtain the equation

$$\int_{\Omega_j} \nabla\psi \cdot \nabla p_H(\lambda_1, \ldots, \lambda_N)\, dx + \sum_{i=1}^{N} \lambda_i \int_{\Omega_i} \nabla\psi \cdot \nabla \left(\frac{\partial p_H}{\partial \lambda_j}(\lambda_1, \ldots, \lambda_N) \right) dx = 0$$

for all $\psi \in V$, or

$$\int_{\Omega} \nabla\psi \cdot (\Lambda_H \nabla q_j)\, dx = -\int_{\Omega_j} \nabla\psi \cdot \nabla p_H(\lambda_1, \ldots, \lambda_N)\, dx \quad \text{for all } \psi \in V, \qquad (2.23)$$

where $q_j = \partial p_H / \partial \lambda_j$. That is, to compute $\partial p_H / \partial \lambda_j$ for $j = 1, \ldots, N$, we have to solve N elliptic PDEs of the form (2.23). However, all these PDEs are very similar. Only the integration area on the right hand side of equation (2.23) differs for the

q_j's. This observation can be exploited by introducing an auxiliary problem. Let the bilinear form $a_{\Lambda_H}(\cdot,\cdot)$ on $V \times V$ be defined as follows

$$a_{\Lambda_H}(\varphi,\psi) = \int_\Omega \nabla\psi \cdot (\Lambda_H \nabla\varphi)\, dx,$$

and recall that $q_j = \partial p_H/\partial\lambda_j$ satisfies

$$a_{\Lambda_H}(q_j,\psi) = -\int_{\Omega_j} \nabla\psi \cdot \nabla p_H(\lambda_1,\ldots,\lambda_N)\, dx \quad \text{for all } \psi \in V, \tag{2.24}$$

cf. equation (2.23). Now, the auxiliary problem is defined as follows: Find $\tau = \tau(\Lambda_H) \in V$ such that

$$a_{\Lambda_H}(\tau,\psi) = \int_\Omega [\Lambda_H \nabla p_H(\Lambda_H), \Lambda_H \Lambda^{-1} \nabla\psi]\, dx \quad \text{for all } \psi \in V. \tag{2.25}$$

Then, from (2.22) and by putting $\psi = q_j$ in (2.25) we find that

$$\begin{aligned}
\frac{\partial J}{\partial \lambda_j} &= 2\lambda_j \int_{\Omega_j} [\nabla p_H(\lambda_1,\ldots,\lambda_N), \Lambda^{-1}\nabla p_H(\lambda_1,\ldots,\lambda_N)]\, dx \\
&\quad +2\int_\Omega [\Lambda_H \nabla p_H(\lambda_1,\ldots,\lambda_N), \Lambda_H\Lambda^{-1}\nabla q_j]\, dx \\
&\quad +2\alpha\lambda_j|\Omega_j| - 2\alpha\int_{\Omega_j} \Lambda\, dx \\
&= 2\lambda_j \int_{\Omega_j} [\nabla p_H(\lambda_1,\ldots,\lambda_N), \Lambda^{-1}\nabla p_H(\lambda_1,\ldots,\lambda_N)]\, dx \\
&\quad +2a_{\Lambda_H}(\tau(\Lambda_H), q_j) + 2\alpha\lambda_j|\Omega_j| - 2\alpha\int_{\Omega_j} \Lambda\, dx.
\end{aligned}$$

Finally, by putting $\psi = \tau(\Lambda_H)$ in (2.24) it follows that

$$\begin{aligned}
\frac{\partial J}{\partial \lambda_j} &= 2\lambda_j \int_{\Omega_j} [\nabla p_H(\lambda_1,\ldots,\lambda_N), \Lambda^{-1}\nabla p_H(\lambda_1,\ldots,\lambda_N)]\, dx \\
&\quad -2\int_{\Omega_j} \nabla\tau(\lambda_1,\ldots,\lambda_N) \cdot \nabla p_H(\lambda_1,\ldots,\lambda_N)\, dx \\
&\quad +2\alpha\lambda_j|\Omega_j| - 2\alpha\int_{\Omega_j} \Lambda\, dx,
\end{aligned} \tag{2.26}$$

where $\tau(\lambda_1,\ldots,\lambda_N) = \tau(\Lambda_H)$. Clearly, from (2.26) it follows that it is sufficient to solve (2.10) and (2.25) in order to compute $\partial J/\partial\lambda_j$ for $j = 1,\ldots,N$. Moreover, the stiffness matrices generated by finite element discretizations of (2.10) and (2.25) are identical, provided that the same discretization is used.

3. Analytical examples. In this section we will present some simple analytical examples illustrating some properties of the weighted output least squares (WOLS) scheme derived above. In the next section we will discuss how to solve the minimization problem (2.20) computationally and some numerical examples will be given in Section 5. However, we will in this section describe some simple cases where the

minimization can be done by hand and where we get explicit expressions for the optimal values of the upscaled permeability. These expression are used to compare the WOLS-method by the less computationally efficient output least squares OLS-method and some simple averaging schemes.

Throughout this section we consider the minimization problem (2.14) in the case of $\alpha = 0$. The upscaling problem is in this case easily seen to not have a unique solution; consider the unique solution of the problem

$$-\nabla \cdot (\lambda \nabla p) = f, \qquad \mathbf{v} \cdot n = 0 \text{ on } \partial\Omega, \qquad \int_\Omega p \, dx = 0,$$

with velocity field given by

$$\mathbf{v} = -\lambda \nabla p.$$

Similarly, we let $\beta > 0$ be a given constant and consider the problem

$$-\nabla \cdot (\beta\lambda \nabla \widetilde{p}) = f, \qquad \widetilde{\mathbf{v}} \cdot n = 0 \text{ on } \partial\Omega, \qquad \int_\Omega \widetilde{p} \, dx = 0,$$

with the velocity field

$$\widetilde{\mathbf{v}} = -\beta\lambda \nabla \widetilde{p}.$$

Then, by uniqueness we have $p = \beta\widetilde{p}$, and thus

$$\widetilde{\mathbf{v}} = -\beta\lambda \nabla \widetilde{p} = -\lambda \nabla p = \mathbf{v}.$$

Hence, two permeability fields λ and $\beta\lambda$ generate exactly the same velocity field. This means that given a fine scale permeability field λ_h, the minimization problem (2.14) can, in the case of $\alpha = 0$, only determine the coarse scale permeability field Λ_h up to multiplication by a positive constant.

This observation can be used to reduce the degrees of freedom in the problem of upscaling. Consider the problem of upscaling from four to two values in the permeability field for the pressure equation defined on the unit square $\Omega = [0,1] \times [0,1]$. In Figure 3.1 we have depicted the data; the "fine-scale" permeability λ_h is given by the values $\lambda_1, \lambda_2, \lambda_3, \lambda_4$ on the elements e_1, e_2, e_3, e_4 respectively. Given these data, we want to compute the optimal values of the "coarse-scale" permeability Λ_H field given by the values Λ_1, Λ_2 on the elements E_1, E_2 respectively, cf. Figure 3.2. Based on the observations above, we can with no loss of generality put

$$\lambda_4 = \Lambda_2 = 1.$$

In both problems the source term is defined by

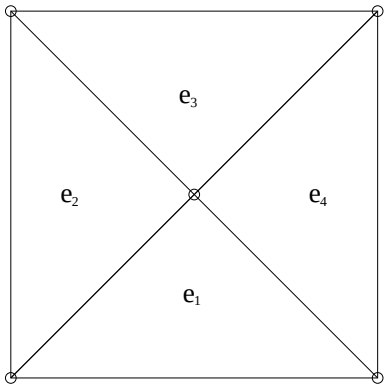

FIG. 3.1. *"Fine-scale" model.*

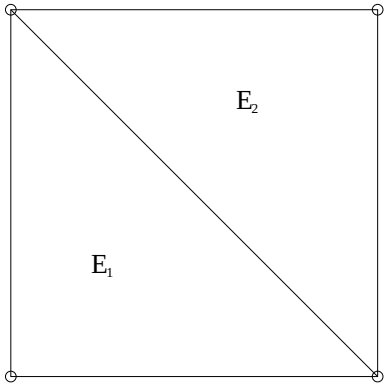

FIG. 3.2. *"Coarse-scale" model.*

$$f(x,y) = \begin{cases} \alpha_0 & \text{for } (x,y) \in S_1 = [0,1/10] \times [4/10,6/10], \\ -\alpha_0 & \text{for } (x,y) \in S_2 = [9/10,1] \times [4/10,6/10], \\ 0 & \text{elsewhere,} \end{cases}$$

where the strength α_0 of the source is given.

By discretizing the "fine-scale" model

$$-\nabla \cdot (\lambda_h \nabla p_h) = f, \qquad \mathbf{v_h} \cdot n = 0 \qquad \int_\Omega p_h \, dx = 0,$$

using linear elements with nodes marked in Figure 3.1, we get the "fine-scale" discrete velocity field defined by

$$\mathbf{v_h}(x,y) = \begin{cases} \frac{2\beta_0\lambda_1}{(\lambda_1+1)(\lambda_1+\lambda_2)} \begin{pmatrix} 2\lambda_1+\lambda_2+1 \\ 1-\lambda_2 \end{pmatrix} & for \quad (x,y) \in e_1, \\ \frac{2\beta_0\lambda_2}{(\lambda_2+\lambda_3)(\lambda_1+\lambda_2)} \begin{pmatrix} \lambda_1+2\lambda_2+\lambda_3 \\ \lambda_3-\lambda_1 \end{pmatrix} & for \quad (x,y) \in e_2, \\ \frac{2\beta_0\lambda_3}{(\lambda_2+\lambda_3)(\lambda_3+1)} \begin{pmatrix} \lambda_2+2\lambda_3+1 \\ \lambda_2-1 \end{pmatrix} & for \quad (x,y) \in e_3, \\ \frac{2\beta_0}{(\lambda_1+1)(\lambda_3+1)} \begin{pmatrix} \lambda_1+\lambda_3+2 \\ \lambda_1-\lambda_3 \end{pmatrix} & for \quad (x,y) \in e_4, \end{cases}$$

where $\beta_0 = 9\alpha_0/1000$, and where we have used $\lambda_4 = 1$. Similarly, by discretizing the "coarse-scale" model

$$-\nabla \cdot (\Lambda_H \nabla p_H) = f, \qquad \mathbf{v_H} \cdot n = 0 \qquad \int_\Omega p_H \, dx = 0,$$

using linear elements with nodes marked in Figure 3.2, we get the "coarse-scale" discrete velocity field defined by

$$\mathbf{v_H}(x,y) = \begin{cases} \frac{\beta_0}{\Lambda+1} \begin{pmatrix} 3\Lambda+1 \\ 1-\Lambda \end{pmatrix} & for \quad (x,y) \in E_1, \\ \frac{\beta_0}{\Lambda+1} \begin{pmatrix} 3+\Lambda \\ \Lambda-1 \end{pmatrix} & for \quad (x,y) \in E_2, \end{cases}$$

where we recall that $\Lambda_2 = 1$ and where we have used $\Lambda = \Lambda_1$ to simplify the notation. Having these expressions for the "fine-scale" and "coarse-scale" velocities, we consider first the Output Least Squares (OLS) approach and seek the minimum of

$$J_{ols}(\Lambda) = \| \mathbf{v_h} - \mathbf{v_H} \|_{(L^2(\Omega))^2}.$$

That is, given λ_1, λ_2 and λ_3, we seek the value of Λ that minimizes J_{ols}. The unique minimum is given by

$$\Lambda_{ols} = \frac{2\lambda_1\lambda_2 + \lambda_1\lambda_3 + \lambda_2}{\lambda_1\lambda_3 + \lambda_2 + 2\lambda_3}.$$

Next we consider the weighted output least squares (WOLS) scheme and thus seek the minimum of

$$J_{wols}(\Lambda) = \int_\Omega [\Lambda \nabla p_H, \lambda^{-1} \Lambda \nabla p_H] \, dx,$$

cf. (2.16) with $\alpha = 0$. The unique minimum of J_{wols} is attained at

$$\Lambda_{wols} = \frac{\lambda_1\lambda_2 + \lambda_1\lambda_2\lambda_3}{\lambda_2\lambda_3 + \lambda_1\lambda_3}.$$

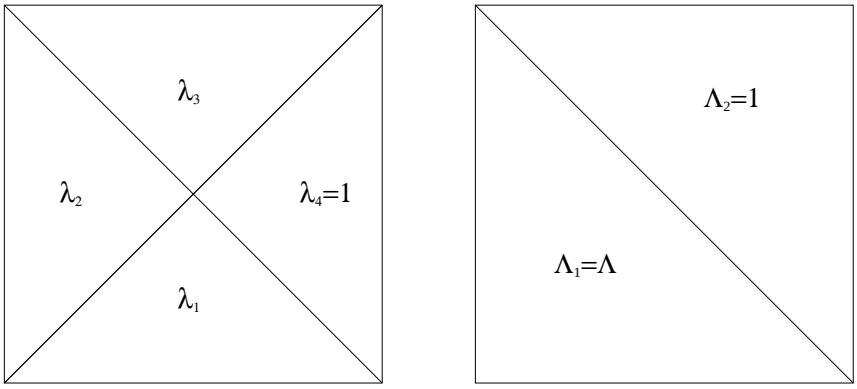

FIG. 3.3. *Upscaling from four to two values. Note that* λ_4 *and* Λ_2 *is chosen to be* 1.

We want to compare these upscaling formulas by similar formulas given by arithmetic, harmonic and geometric averaging for the upscaling problem defined in Figure 3.3. In the following Table we compare the five upscaling schemes for some different data; note that in these cases ε is assumed to be a small ($\varepsilon \ll 1$) positive constant and we have chosen $\lambda_3 = 1$.

General	$\lambda_1 = 1-\varepsilon$, $\lambda_2 = 1+\varepsilon$	$\lambda_1 = \varepsilon$, $\lambda_2 = 1$	$\lambda_1 = \varepsilon$, $\lambda_2 = 1/\varepsilon$
$\Lambda_{arit} = \frac{1}{2}(\lambda_1+\lambda_2)$	1	$\frac{1}{2}(\varepsilon+1) \approx 1/2$	$\frac{1}{2}(\varepsilon+1/\varepsilon) \approx \frac{1}{2\varepsilon}$
$\Lambda_{harm} = 2\frac{\lambda_1\lambda_2}{\lambda_1+\lambda_2}$	$1-\varepsilon^2$	$2\frac{\varepsilon}{\varepsilon+1} \approx 2\varepsilon$	$2\frac{\varepsilon}{\varepsilon^2+1} \approx 2\varepsilon$
$\Lambda_{geom} = \sqrt{\lambda_1\lambda_2}$	$\sqrt{1-\varepsilon^2} \approx 1-\frac{1}{2}\varepsilon^2$	$\sqrt{\varepsilon}$	1
$\Lambda_{ols} = \frac{2\lambda_1\lambda_2+\lambda_1\lambda_3+\lambda_2}{\lambda_1\lambda_3+\lambda_2+2\lambda_3}$	$1-\frac{1}{2}\varepsilon^2$	$\frac{3\varepsilon+1}{\varepsilon+3} \approx 1/3$	1
$\Lambda_{wols} = \frac{\lambda_1\lambda_2+\lambda_1\lambda_2\lambda_3}{\lambda_2\lambda_3+\lambda_1\lambda_3}$	$1-\varepsilon^2$	$2\frac{\varepsilon}{\varepsilon+1} \approx 2\varepsilon$	$2\frac{\varepsilon}{\varepsilon^2+1} \approx 2\varepsilon$

We observe from this table that:

- For small jumps, all the methods produce almost identical results.
- All the methods reproduce a constant permeability.
- The results of the five methods vary significantly for permeabilities with large jumps. This issue will be analyzed further in the numerical experiments presented below.
- As expected from the definition of the WOLS-method, it emphasizes the low permeable zones and should therefore be applicable when it is desired to reproduce such regions in the upscaled permeability field.
- For the simple example presented here, the harmonic averaging and the WOLS-method produce identical results. We will discuss this issue further below.

4. A fix-point algorithm. The purpose of this section is to present a simple algorithm for computing the minimum point Λ_e of the cost-functional $J(\cdot)$, defined in

(2.20). Clearly, the optimization problem

$$\min_{\Lambda_H \in Q} J(\Lambda_H) \tag{4.1}$$

is non-linear, and hence non-trivial. This sort of problem can be solved by one of the standard minimization methods, like Newton's method or the conjugate gradient method, cf. e.g. Fletcher [16]. However, for the sake of simplicity, we will apply a fix-point algorithm to compute the stationary point of $J(\cdot)$. This method is easy to implement and proved to be efficient enough to solve our test problems, cf. Section 5. However, it should be noted that large scale applications of our scheme would require the implementation of faster methods for solving this minimization problem.

Our algorithm is based on formula (2.26) for the partial derivatives of $J(\cdot)$. More precisely, from equation (2.26) we find the following condition for a minimum point $\lambda_1, \ldots, \lambda_N$ of $J(\cdot)$,

$$\frac{\partial J}{\partial \lambda_j}(\lambda_1, \ldots, \lambda_N) = 0$$

and thus

$$\lambda_j = \frac{\int_{\Omega_j} \nabla\tau(\lambda_1, \ldots, \lambda_N) \cdot \nabla p_H(\lambda_1, \ldots, \lambda_N)\, dx + \alpha \int_{\Omega_j} \Lambda\, dx}{\int_{\Omega_j} [\nabla p_H(\lambda_1, \ldots, \lambda_N), \Lambda^{-1} \nabla p_H(\lambda_1, \ldots, \lambda_N)]\, dx + \alpha |\Omega_j|}.$$

Based on this observation we now define the following fix-point algorithm to compute approximations $\Lambda_H^{(0)}$, $\Lambda_H^{(1)}$, $\Lambda_H^{(2)}$,..., $\Lambda_H^{(n)}$,..., of the effective permeability Λ_e, i.e. approximations of the solution of (4.1).

Algorithm 1.

1. for $i = 1, \ldots, N$ do
   (a) define $\lambda_i^{(0)}$
2. for $n = 0, \ldots,$ *until convergence* do
   (a) Compute $p_H(\lambda_1^{(n)}, \ldots, \lambda_N^{(n)})$ by solving the following problem: Find $p_H(\lambda_1^{(n)}, \ldots, \lambda_N^{(n)}) = p_H(\Lambda_H^{(n)}) \in V$ such that

$$\int_\Omega \nabla\psi \cdot (\Lambda_H^{(n)} \nabla p_H(\Lambda_H^{(n)}))\, dx = \int_\Omega f\psi\, dx \quad \text{for all } \psi \in V.$$

   (b) Compute $\tau(\lambda_1^{(n)}, \ldots, \lambda_N^{(n)})$ by solving the following problem: Find $\tau(\lambda_1^{(n)}, \ldots, \lambda_N^{(n)}) = \tau(\Lambda_H^{(n)}) \in V$ such that

$$\int_\Omega \nabla\psi \cdot (\Lambda_H^{(n)} \nabla\tau(\Lambda_H^{(n)}))\, dx = \int_\Omega [\Lambda_H^{(n)} \nabla p_H(\Lambda_H^{(n)}), \Lambda_H^{(n)} \Lambda^{-1} \nabla\psi]\, dx$$

   for all $\psi \in V$.
   (c) if $\alpha = 0$ then

$stop = N - 1$

$\lambda_N^{(n+1)} = \lambda_N^{(0)}$

else $stop = N$.

(d) for $i = 1, \ldots, stop$ do

$$\lambda_i^{(n+1)} = \frac{\int_{\Omega_i} \nabla\tau(\lambda_1^{(n)}, \ldots, \lambda_N^{(n)}) \cdot \nabla p_H(\lambda_1^{(n)}, \ldots, \lambda_N^{(n)})\, dx + \alpha \int_{\Omega_i} \Lambda\, dx}{\int_{\Omega_i} [\nabla p_H(\lambda_1^{(n)}, \ldots, \lambda_N^{(n)}), \Lambda^{-1} \nabla p_H(\lambda_1^{(n)}, \ldots, \lambda_N^{(n)})]\, dx + \alpha |\Omega_i|}.$$

Recall that if $\alpha = 0$ then the problem (2.16) does not have a unique solution, see Section 3. In **Algorithm 1** this problem is handled by putting $\lambda_N^{(n)} = \lambda_N^{(0)}$ for all n.

5. Numerical experiments. In this section we present some numerical examples illustrating the behavior of the upscaling technique presented above. Consider the fine scale pressure equation (2.2)-(2.3) and recall that in each experiment we need to specify the solution domain Ω, the source term f and the (fine scale) absolute permeability Λ. In addition, a set of coarse scale grid blocks $\{\Omega_i\}_{i=1}^N$ satisfying (2.5) has to be defined.

In all the experiments presented below, the solution domain is given by $\Omega = (0,3) \times (0,3)$, and, if not stated otherwise, the source term is given by

$$f(x,y) = \begin{cases} 1 & \text{for } (x,y) \in (12/32, 15/32) \times (18/32, 21/32), \\ -1 & \text{for } (x,y) \in (84/32, 87/32) \times (78/32, 81/32), \\ 0 & \text{elsewhere.} \end{cases} \tag{5.1}$$

That is, there is one injection well and one production well located close to the lower left corner and upper right corner of the reservoir, respectively. Note that this particular f satisfies condition (2.11). Obviously, in order to implement **Algorithm 1**, equations of the form (2.10) and (2.25) have to be solved numerically, cf. steps 2a and b in **Algorithm 1**. In this paper these equations are solved by the finite element method. If not stated otherwise, we apply standard piecewise linear finite elements. In all the experiments, the finite elements are used as coarse grid-blocks $\{\Omega_i\}_{i=1}^N$. All the implementation is done within the Diffpack framework, cf. [10] and Langtangen [22]. The pressure equation (2.10) and the auxiliary problem (2.25) are solved using the Conjugate Gradient method in conjunction with the precondition technique studied in [7].

5.1. Case I: A simple test problem. First, we want to check that our method produce reasonable results for simple smooth permeability functions. In this experiment the absolute permeability Λ is given by

$$\Lambda(x,y) = 1.5 + \sin(6\pi xy) \quad \text{for } (x,y) \in \Omega,$$

i.e. Λ is smooth and has small variation. The coarse grid-blocks $\{\Omega_i\}_{i=1}^N$ are defined in terms of a uniform 32×32 triangular mesh on Ω. The effective permeability Λ_e is computed by **Algorithm 1**, applying the arithmetic average as initial guess,

$$\lambda_j^{(0)} = \frac{1}{|\Omega_j|} \int_{\Omega_j} \Lambda(x)\, dx \quad \text{for } j = 1, \ldots, N.$$

The iteration was halted when

$$|J(\Lambda_H^{(n)}) - J(\Lambda_H^{(n-1)})| \leq 10^{-9}.$$

Putting $\alpha = 0$, this stopping-criterion was fulfilled after 8 iterations. Figure 5.1 shows the velocity fields generated by our WOLS-method and the arithmetic average, and the velocity field obtained by solving the fine scale pressure equation (2.9). The latter was solved on a uniform 128×128 triangular mesh. We see that both the arithmetic average and the WOLS-method produce reasonable results in this case. Furthermore, Table 5.1 shows that the value of the cost-functional $J(\cdot)$ is almost identical for the arithmetic average and for the effective permeability Λ_e generated by the WOLS-method. Hence, since the arithmetic average is known to produce accurate results for simple smooth permeability functions, we conclude that also the WOLS-method seems to handle this sort of problems adequately.

method	J
arithmetic average	$1.20978 * 10^{-4}$
weighted output least squares (WOLS)	$1.20756 * 10^{-4}$

TABLE 5.1

The table shows the function values of the cost-functional $J(\cdot)$ for Case I.

5.2. Case II: A reservoir containing a barrier. Next, we consider a reservoir containing a low-permeable region. This low-permeable zone is located close to the center of the reservoir and has the shape of a thin rectangle, see Figure 5.2. On the coarse scale level this barrier is not resolved. More precisely, the absolute permeability Λ is defined as follows

$$\Lambda(x, y) = \begin{cases} \delta & \text{for } (x, y) \in [15.5 * 3/32, 16 * 3/32] \times [3 * 3/32, 29 * 3/32], \\ 1 & \text{elsewhere,} \end{cases}$$

where δ is a small positive parameter. For this problem it turned out to be possible to solve (2.16) with $\alpha = 0$, by computing the effective permeability for a decreasing sequence of δ; $\delta = 0.016, 0.015, 0.014, \ldots, 0.004$. For each value of δ the approximation of the effective permeability from the previous value of δ is used as start vector

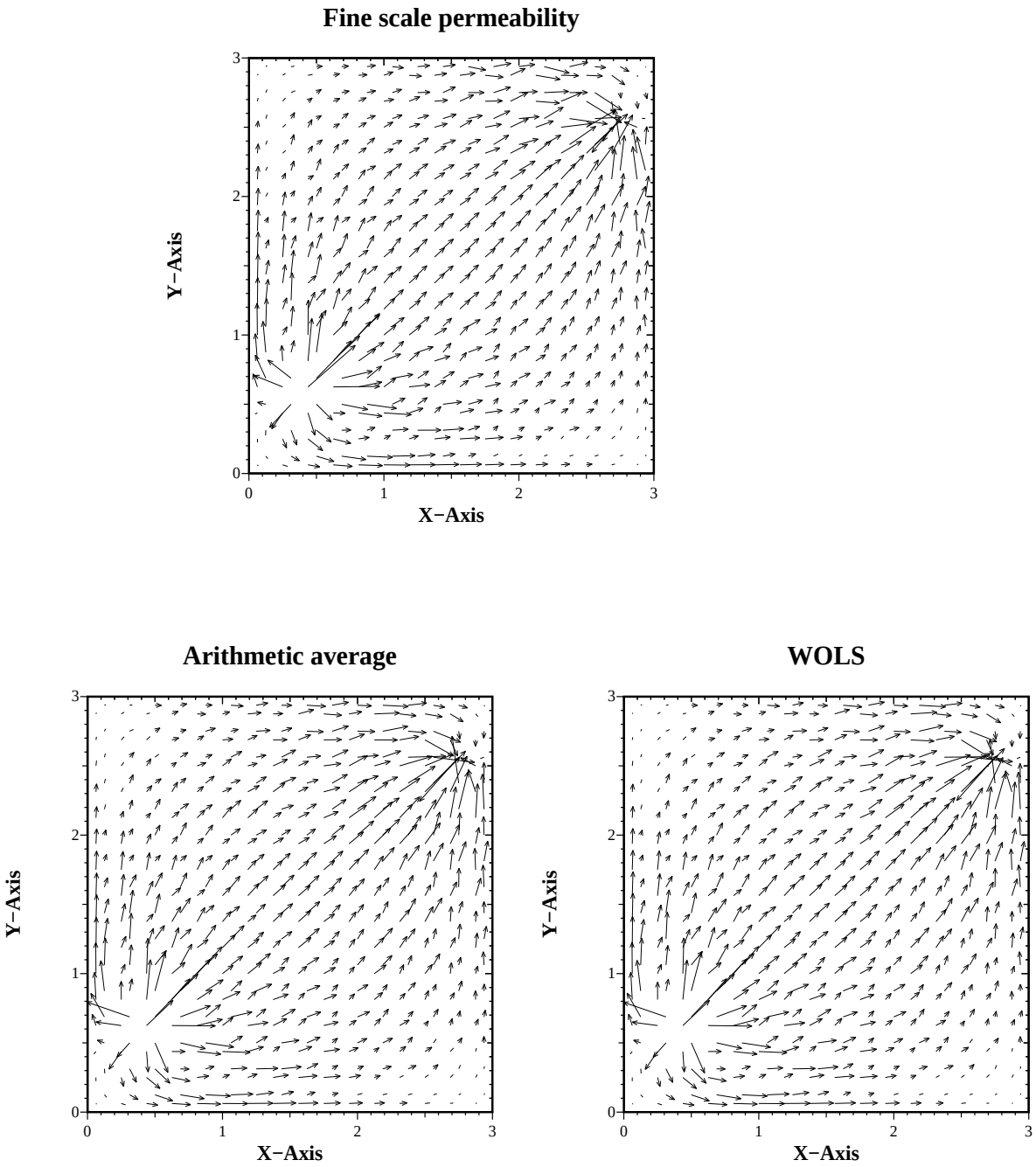

FIG. 5.1. *The figure shows the velocity fields for the problem described in Case I; upscaling of a smooth permeability field.*

in **Algorithm 1**. For $\delta = 0.016$ the arithmetic average was used as initial guess. Applying the stopping-criterion

$$|J(\Lambda_H^{(n)}) - J(\Lambda_H^{(n-1)})| \leq 10^{-8},$$

Algorithm 1 converged in 4-8 iterations, for each value of δ.

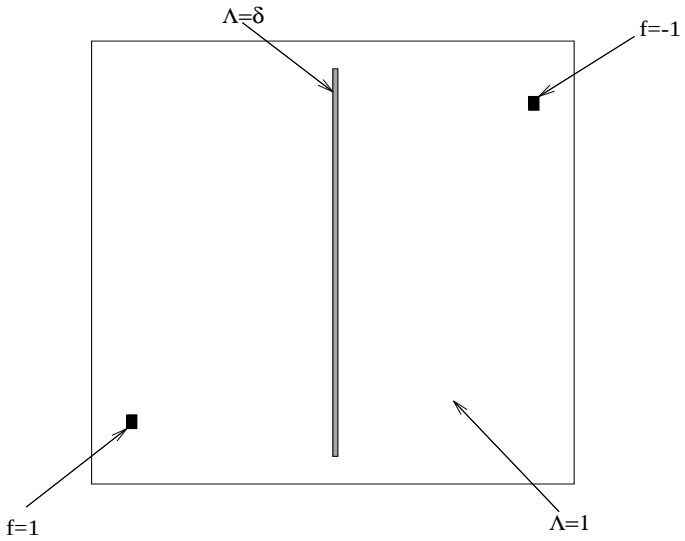

FIG. 5.2. *The geometry of the reservoir used in Case II.*

Figure 5.3 shows the numerical results computed on a uniform 32×32 triangular coarse grid. Comparing the results with the velocity field computed on the fine grid (a uniform 64×64 triangular mesh) we see that the WOLS-method produce far better results than the arithmetic average. We also observe that the geometric average produce a reasonable permeability field in this case. However, if a uniform 16×16 triangular coarse grid is applied, then both the arithmetic average and the geometric average fail to solve this problem, cf. Figure 5.4, whereas the WOLS-method produce an appropriate velocity field. From Table 5.2 and Table 5.3 we observe that the function value of $J(\cdot)$ is smaller for the WOLS-method than for the simple averaging schemes. We conclude that the results of this example suggest that the WOLS-scheme gives a more accurate representation of tiny low-permeable zones than the simple averaging schemes can produce.

method	J
arithmetic average	$2.53108 * 10^{-4}$
geometric average	$2.43801 * 10^{-4}$
weighted output least squares (WOLS)	$1.85891 * 10^{-4}$

TABLE 5.2

The table shows the function values, computed on a uniform 32×32 *triangular grid, of the cost-functional* $J(\cdot)$ *for Case II.*

5.3. Case III: A reservoir containing a barrier and a channel. The geometry of the reservoir considered in this example is similar to the one studied in Case

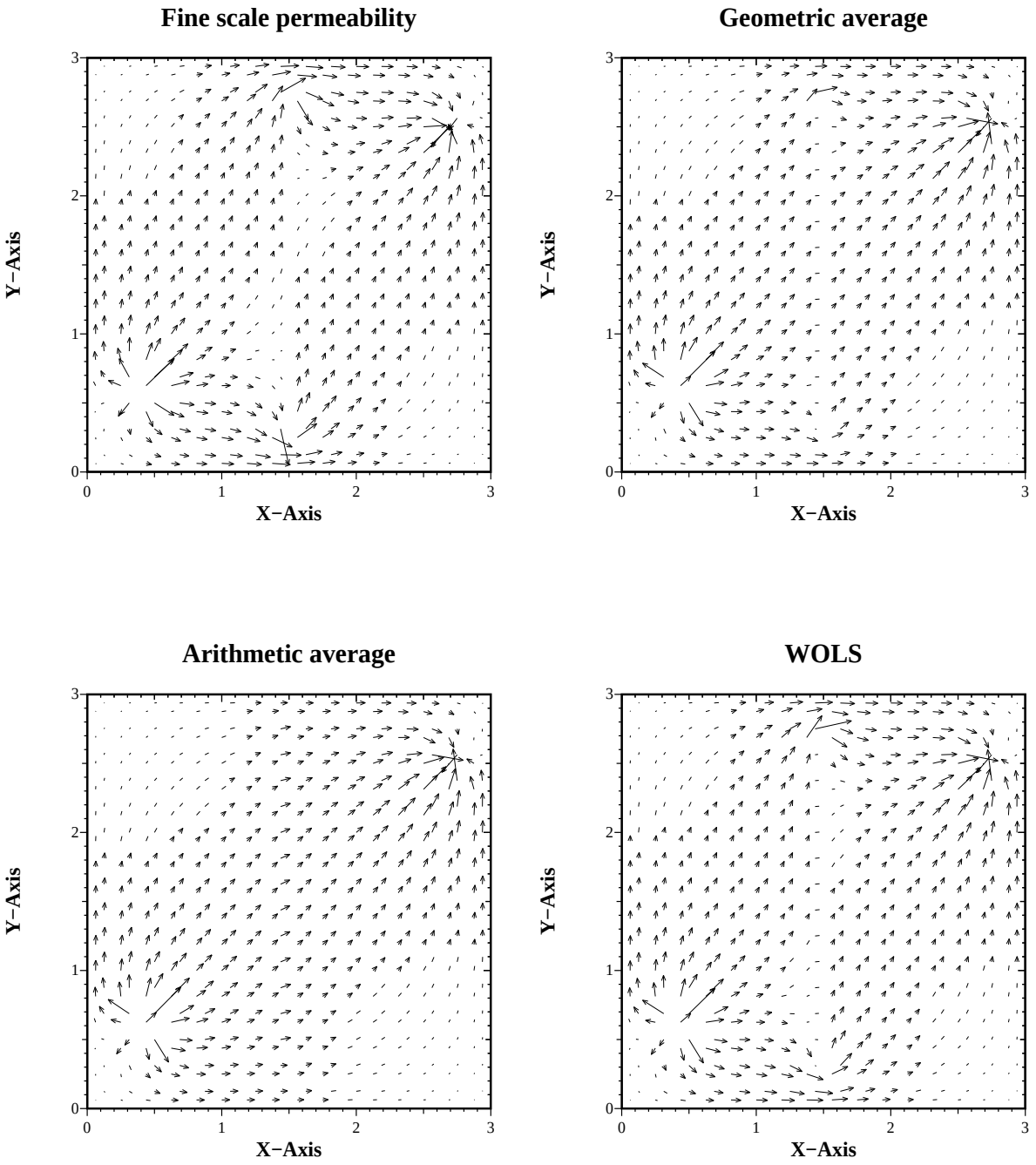

FIG. 5.3. *The figure shows the fine scale velocity field and the coarse scale velocity fields for Case II; upscaling from a* 64×64 *to a* 32×32 *mesh.*

II. To challenge our upscaling technique we consider a reservoir with a low-permeable and a high-permeable zone located next to each other, see Figure 5.5. This structure is positioned such that it is not resolved in the uniform 32×32 triangular coarse grid. In this problem the absolute permeability Λ is defined on a uniform 64×64 triangular

method	J
arithmetic average	$8.55107 * 10^{-4}$
geometric average	$7.44147 * 10^{-4}$
weighted output least squares (WOLS)	$4.32617 * 10^{-4}$

TABLE 5.3

The table shows the function values, computed on a uniform 16×16 *triangular grid, of the cost-functional* $J(\cdot)$ *for Case II.*

grid as follows

$$\Lambda(x,y) = \begin{cases} \delta & \text{for } (x,y) \in [15*3/32, 15.5*3/32] \times [3*3/32, 29*3/32], \\ 1/\delta & \text{for } (x,y) \in (15.5*3/32, 16*3/32] \times [3*3/32, 29*3/32], \\ 1 & \text{elsewhere,} \end{cases}$$

for a small $\delta > 0$. Again, by computing the effective permeability for several values of δ, $\delta = 0.05, 0.04, \ldots, 0.01, 0.009, 0.008, \ldots, 0.005$, we were able to solve the optimization problem (2.16) with zero regularization, i.e. $\alpha = 0$. For each value of δ, 6-11 iterations were needed to fulfill the stopping-criterion

$$|J(\Lambda_H^{(n)}) - J(\Lambda_H^{(n-1)})| \leq 10^{-8}.$$

Figure 5.6 shows that both the effective permeability computed by the geometric and arithmetic average fail to produce a correct flow picture in this case. However, the WOLS-method solves this problem adequately. Moreover, in Table 5.4 we observe that the function value of the cost-functional $J(\cdot)$ is again smaller for the WOLS-method than for the geometric and arithmetic average.

method	J
arithmetic average	$8.49975 * 10^{-3}$
geometric average	$4.07199 * 10^{-4}$
weighted output least squares (WOLS)	$1.81866 * 10^{-4}$

TABLE 5.4

The table shows the function values of the cost-functional $J(\cdot)$ *for Case III.*

5.4. Case IV: A reservoir containing a channel. The geometry of the reservoir considered in this experiment is depicted in Figure 5.7. More precisely, the source term f is given by

$$f(x,y) = \begin{cases} 1 & \text{for } (x,y) \in (15.5*3/32, 16.5*3/32) \times (6*3/32, 7*3/32), \\ -1 & \text{for } (x,y) \in (28*3/32, 29*3/32) \times (26*3/32, 27*3/32), \\ 0 & \text{elsewhere,} \end{cases}$$

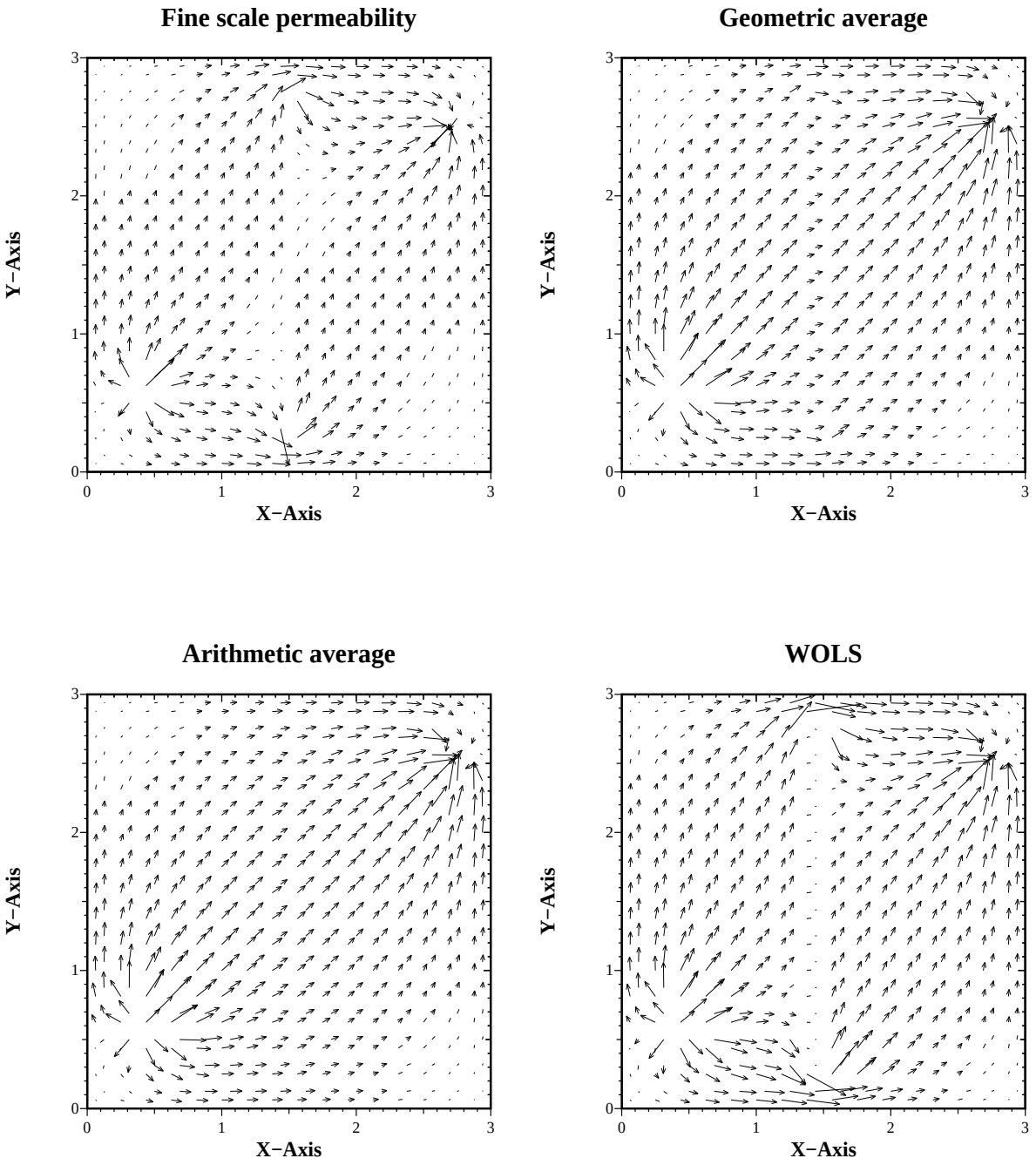

FIG. 5.4. *The figure shows the fine scale velocity field and the coarse scale velocity fields for Case II; upscaling from a* 64×64 *to a* 16×16 *mesh.*

and the absolute permeability Λ is defined as follows

$$\Lambda(x,y) = \begin{cases} 10 & \text{for } (x,y) \in [15.5 * 3/32, 16 * 3/32] \times [10 * 3/32, 20 * 3/32], \\ 0.1 & \text{for } (x,y) \in (0, 15.5 * 3/32) \cup (16 * 3/32, 3) \times [10 * 3/32, 20 * 3/32], \\ 1 & \text{elsewhere.} \end{cases}$$

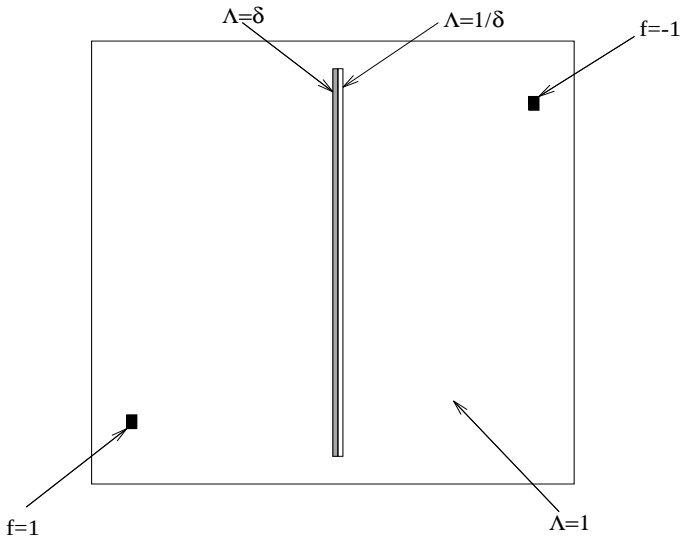

FIG. 5.5. *The structure of the reservoir used in Case III.*

That is, the reservoir contains a high-permeable zone acting as a channel.

In this example we applied bilinear shape functions defined on quadratic elements in the finite element discretizations of equations (2.10) and (2.25), cf. steps 2a and b in **Algorithm 1**. To compute the effective permeability Λ_e, the optimization problem (2.16) was solved for several values of the regularization parameter α, $\alpha = 1, 1/2, 1/4, \ldots, 1/64$. For every value of α, the previously computed solution of (2.16) was used as start vector in **Algoritm 1**. It turned out to be impossible to solve (2.16) with zero regularization using **Algorithm 1**. For $\alpha < 1/64$ the algorithm diverged. In this case a stopping-criterion of the form

$$\|\Lambda_H^{(n)} - \Lambda_H^{(n-1)}\|_{L^\infty(\Omega)} \leq 0.01 \tag{5.2}$$

proved to be suitable to obtain convergence. By using the stopping-criterion applied above, the number of iterations needed to get convergence was much higher. For each value of α, the stopping-criterion (5.2) was fulfilled after 2-5 iterations. The coarse and fine scale grids were defined as uniform 32×32 and 64×64 meshes on Ω, respectively.

Figure 5.8 shows that both the effective permeability computed by the WOLS-method and the effective permeability defined by the arithmetic average produce reasonable flow pictures in this case, but the harmonic average fails to solve this problem. Recall that in Section 3 we observed that the harmonic average and the WOLS-method produced identical results for some analytical examples. In general, these methods do not define identical coarse scale permeabilities, in the present experiment the results computed by the WOLS-scheme differs significantly from the

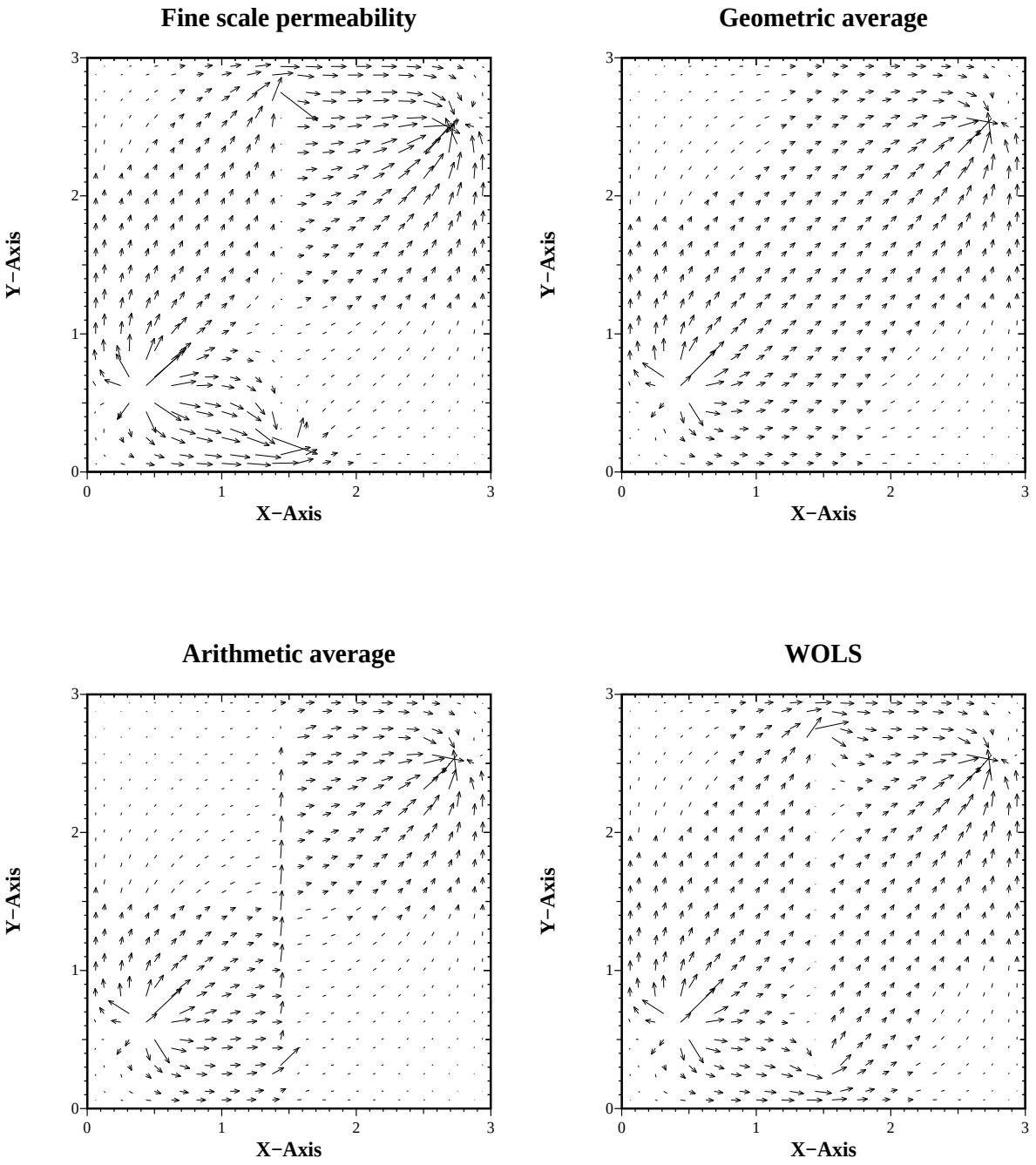

FIG. 5.6. *The figure shows the fine scale velocity field and the coarse scale velocity fields for Case III; upscaling from a* 64×64 *to a* 32×32 *mesh.*

results obtained by the harmonic mean. These observations are confirmed by Table 5.5.

It should be mentioned that the WOLS-method seems to produce more accurate results for low-permeable zones than for high-permeable zones, cf. the computational results in the cases II-IV above. This property of our upscaling technique has been ob-

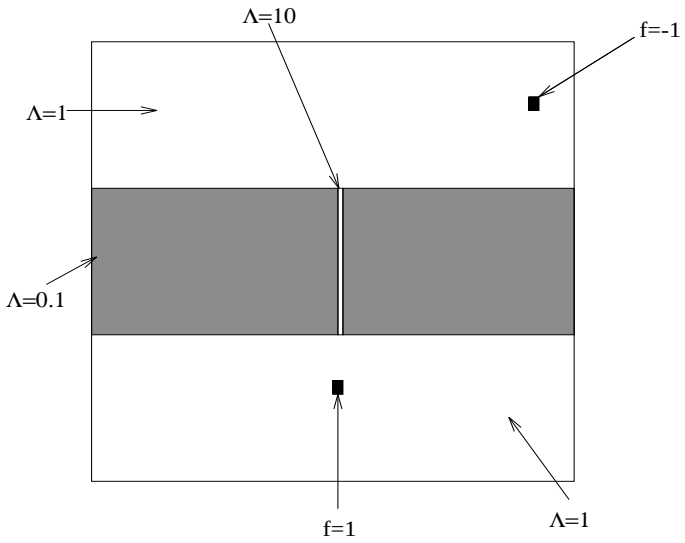

FIG. 5.7. *The geometry of the reservoir used in Case IV.*

method	J
arithmetic average	$3.48076 * 10^{-2}$
harmonic average	$1.60845 * 10^{-1}$
weighted output least squares (WOLS)	$3.45819 * 10^{-2}$

TABLE 5.5

The table shows the function values of the cost-functional $J(\cdot)$ for Case IV.

served in several experiments, and can be explained as follows; recall that the inverse of the absolute permeability Λ^{-1} is applied as weight-function in the definition of the $\|\cdot\|_{\Lambda^{-1}}$-norm, cf. (2.15). The effective permeability Λ_e, defined by the WOLS-method, is determined such that the difference, measured in the $\|\cdot\|_{\Lambda^{-1}}$-norm, between the fine scale velocity field and the coarse scale velocity field is minimized. Hence, in a low permeable zone, where Λ is close to zero and Λ^{-1} is large, the WOLS-method is likely to produce accurate permeability fields.

5.5. Case V: Permeability fields generated by lognormal distributions. In this section we will study permeability fields generated by lognormal distributions. Data of this kind is frequently used as input to reservoir simulators, cf. e.g. [23, 28], and should therefore provide interesting and challenging test problems.

In all the examples presented below, we apply a lognormal distribution with mean value $e^{1/2}$ and variance $e^2 - e$ to produce the fine scale permeability fields. As in the previous section, equations (2.10) and (2.25) are discretized by the finite element method using bilinear shape functions defined on quadratic elements. The effective

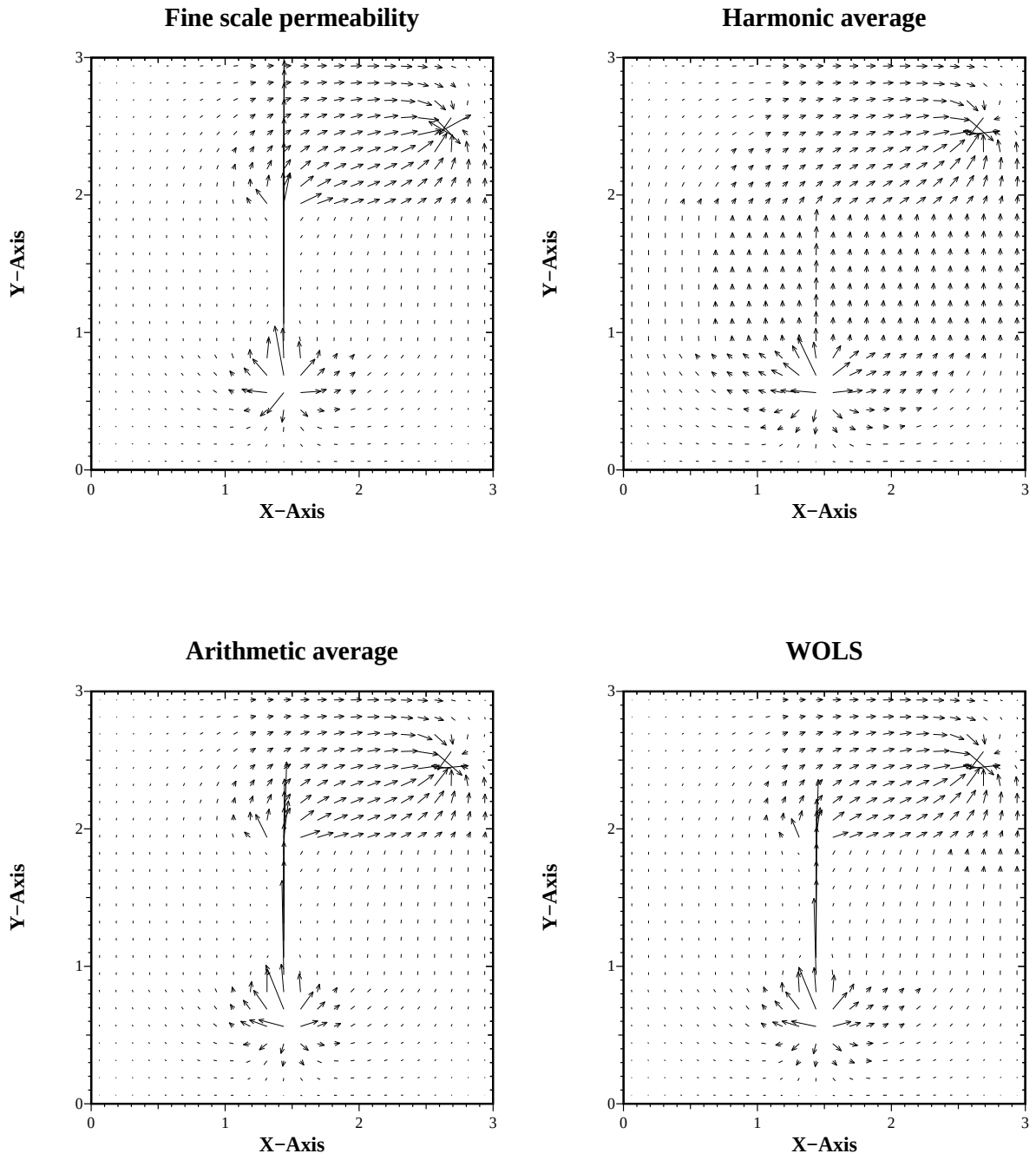

FIG. 5.8. *The figure shows the fine scale velocity field and the coarse scale velocity fields for Case IV; upscaling from a* 64×64 *to a* 32×32 *mesh.*

permeability Λ_e was computed by solving problems of the form (2.20) for a decreasing sequence of regularization parameters; $\alpha = 0.01,\ 0.005,\ 0.0025, \ldots, 7.8125 \cdot 10^{-5}$. For each value of α, a stopping-criterion of the form

$$\|\Lambda_H^{(n)} - \Lambda_H^{(n-1)}\|_{L^\infty(\Omega)} \leq 0.001$$

was used to terminate **Algorithm 1**. It turned out that, if the approximation of the effective permeability obtained for the previous value of α was used as start vector in **Algorithm 1**, then this convergence criterion was fulfilled after 2-17 iterations. In these experiments we used a source term of the form (5.1), and the permeability data was scaled up from a 64×64 mesh to a 32×32 grid.

Finally, it should be mentioned that the input lognormal data was generated by the software package CONTSIM developed at the Norwegian Computing Center (*http://www.nr.no/sand/prj/contsim.html*).

5.5.1. Case V a). In this experiment the correlation length of the fine scale data is 1.0 in both the horizontal and vertical direction. Thus, since the domain of the reservoir is $\Omega = (0,3) \times (0,3)$, we consider a rather smooth permeability field. For such problems, any "reasonable" and well-defined upscaling method should produce acceptable results, cf. Figure 5.9 and Table 5.6.

method	J
arithmetic average	$4.0650 * 10^{-4}$
weighted output least squares (WOLS)	$4.0613 * 10^{-4}$

TABLE 5.6

The table shows the function values of the cost-functional $J(\cdot)$ for Case V a).

5.5.2. Case V b). To challenge our upscaling method we now study permeability data with correlation length 0.1 and 2.0 in the horizontal and vertical direction, respectively. That is, the reservoir has a layered structure: rapid variation in the permeability field in the horizontal direction and slow variation in the vertical direction. In this case, it is difficult to identify any proper flow pattern. The picture looks rather chaotic, see Figure 5.10. It seems like both the coarse scale permeability field defined by the arithmetic average and WOLS tend to smooth the fine scale data. Both methods handle this problem adequately and they produce almost identical results, cf. Table 5.7.

method	J
arithmetic average	$2.0586 * 10^{-3}$
weighted output least squares (WOLS)	$2.0526 * 10^{-3}$

TABLE 5.7

The table shows the function values of the cost-functional $J(\cdot)$ for Case V b).

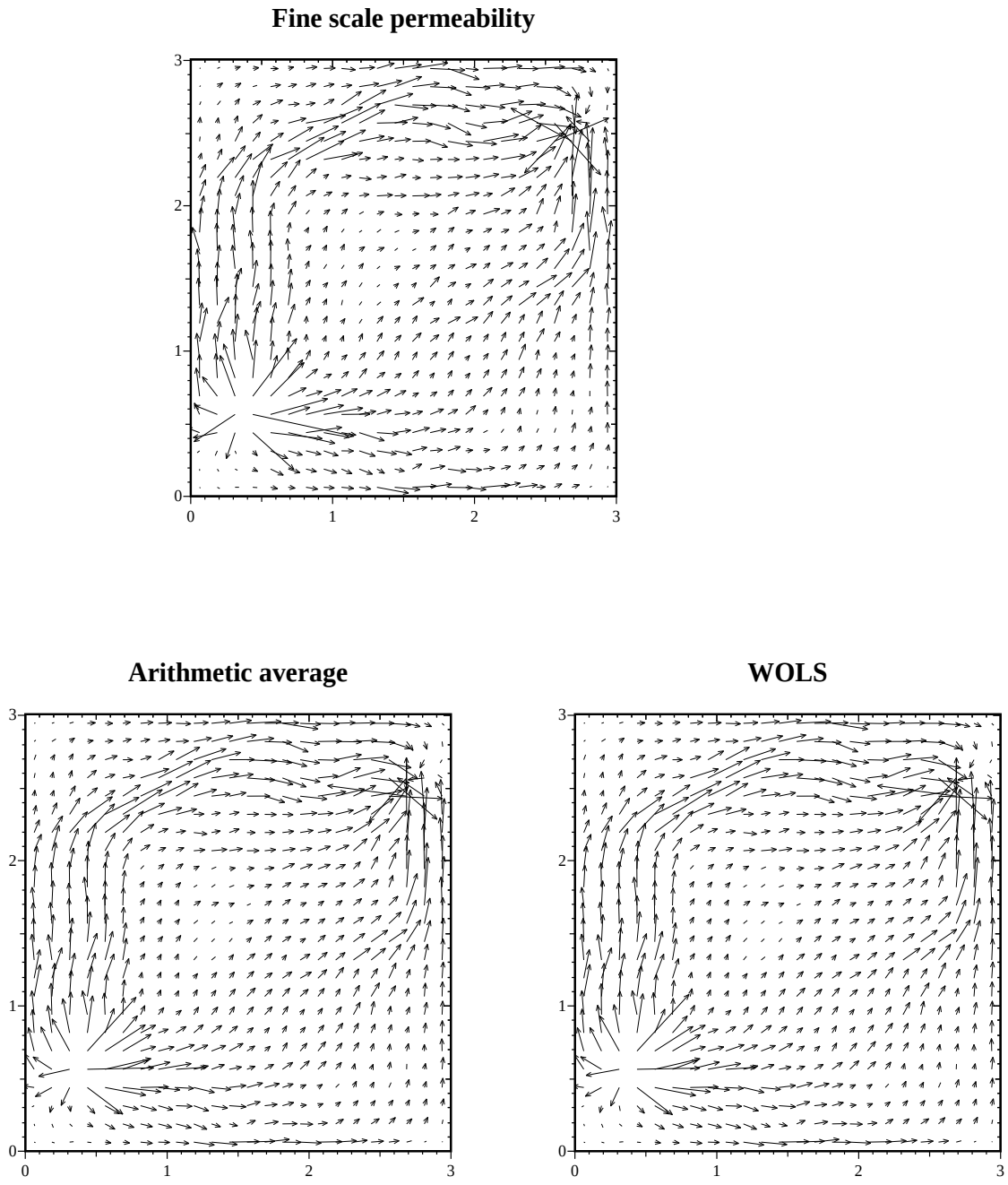

FIG. 5.9. *The figure shows the velocity fields for the problem studied in Case V a); upscaling from a* 64×64 *to a* 32×32 *mesh.*

5.5.3. Case V c). Consider again the permeability data studied in Case V b). What will happen if a barrier is positioned close to the injection well? More precisely, we "re-scaled", by a factor 0.001, the fine scale permeability field in the region

$$S = \{(x, y) \in \Omega;\ 0 < x < 1.5 \text{ and } 8.5 * 3/32 \leq y < 9 * 3/32\}.$$

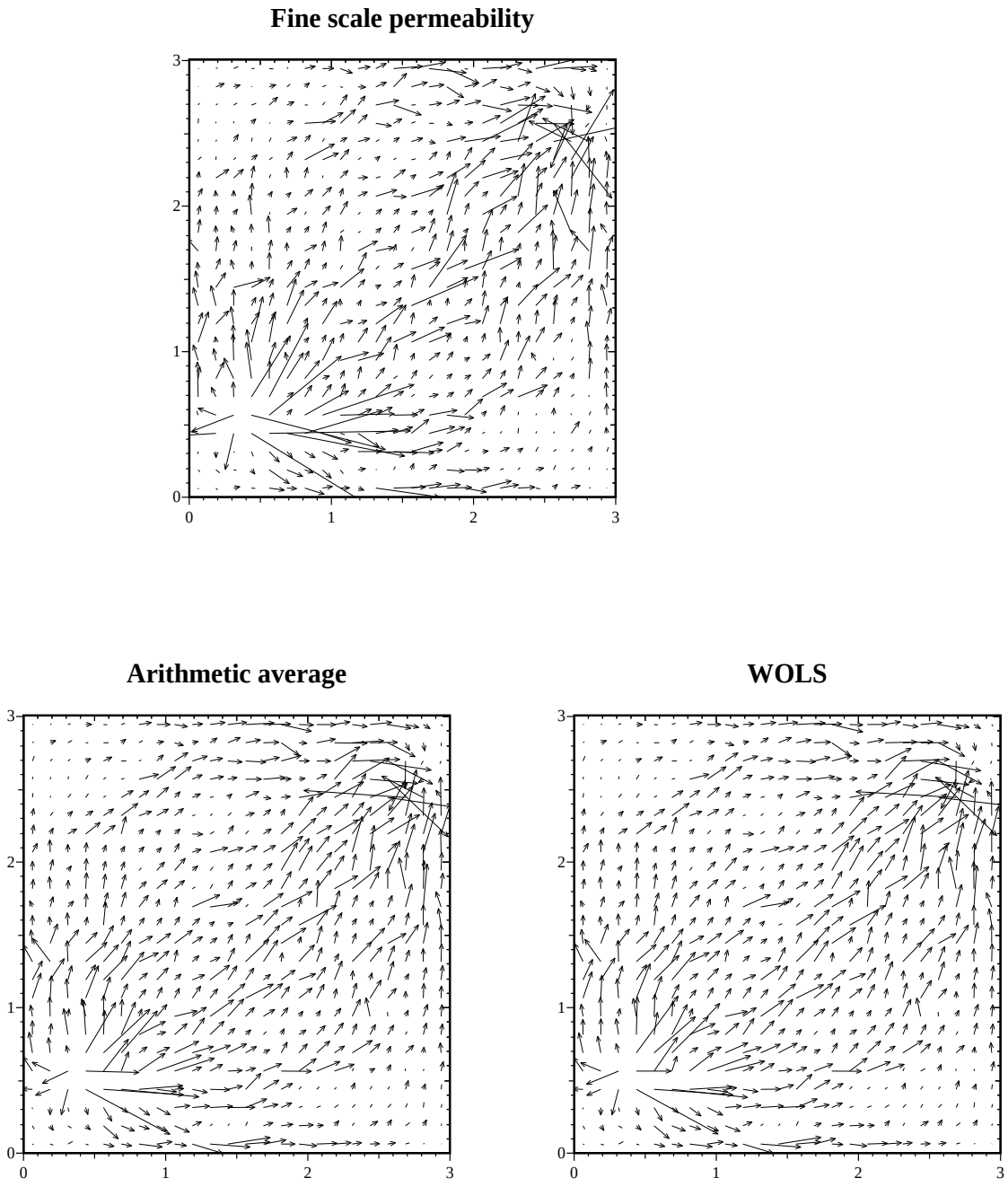

FIG. 5.10. *The figure shows the velocity fields for the problem studied in Case V b); upscaling from a* 64×64 *to a* 32×32 *mesh.*

That is, the permeability is of order 0.001 in S. Notice that the low permeable zone S is not resolved on the coarse scale grid (a 32×32 uniform mesh). Clearly, this barrier introduces a definite flow pattern to our test problem, see Figure 5.11. As expected, in this case the WOLS-method produces far better results than the arithmetic average, cf. also Table 5.8.

method	J
arithmetic average	$4.7970 * 10^{-3}$
weighted output least squares (WOLS)	$2.1832 * 10^{-3}$

TABLE 5.8

The table shows the function values of the cost-functional $J(\cdot)$ for Case V c).

6. Concluding remarks. We have introduced a new upscaling technique for one-phase flow in heterogeneous reservoirs. The method computes an upscaled permeability which minimize, in proper norms, the difference between the fine scale and the coarse scale velocity field. No relation between the fine scale grid and the coarse scale grid is assumed. Moreover, the method does not require the solution of the fine scale pressure equation. Through a series of analytical examples and numerical experiments we have seen that the method produce accurate results for several test problems.

Acknowledgements. The authors want to thank Dr. L. Holden, Prof. H. W. Engl, Dr. T. Gimse and Dr. F. E. Benth for valuable discussions on the work presented in this paper. We would also like to thank X. Cai for answering numerous questions about the Diffpack library, K. Heggland for providing the permeability data used in section 5.5 and the Norwegian Computing Center for their financial support.

REFERENCES

[1] G. ALLAIRE AND F. MURAT, *Homogenization of the Neumann problem with nonisolated holes*, Asymptotic Anal. 7, No.2, 81-95, 1993.

[2] G. ALLAIRE, E. BONNETIER, G. FRANCFORT AND F. JOUVE, *Shape optimization by the homogenization method*, Numer. Math. 76, No.1, 27-68, 1997.

[3] I. BABUSKA, *Homogenization and its application. Mathematical and computational problems*, Num. Sol. of Part. Diff. Eqn.-III, B. Hubbard, ed., Academic Press, N.Y., pp. 89–116, 1976.

[4] H. T. BANKS AND K. KUNISCH, *Estimation techniques for distributed parameter systems*, Birkhäuser, 1989.

[5] A. BENSOUSSAN, J. L. LIONS AND G. PAPANICOLAOU, *Asymptotic analysis for periodic structures*, North-Holland, Amsterdam, 1978.

[6] A. BOURGEAT, E. MARUSVSIĆ AND A. MIKELIĆ, *Effective behaviour of a porous medium containing a thin fissure*, in "Calculus of varitions, homogenization and continuum mechanics", ed. G. Bouchitté, G. Buttazzo, P. Suquet, World Sci., pp. 69–83. 1994.

[7] X. CAI, B. F. NIELSEN AND A. TVEITO, *An analysis of a preconditioner for the discretized pressure equation arising in reservoir simulation*, Preprint 1995-4 at The Department of Informatics, University of Oslo.

[8] R. DAUTRAY AND J.-L. LIONS, *Mathematical Analysis and Numerical Methods for Science and Technology*, vol. II: Functional and Variational Methods, Springer-Verlag, 1988.

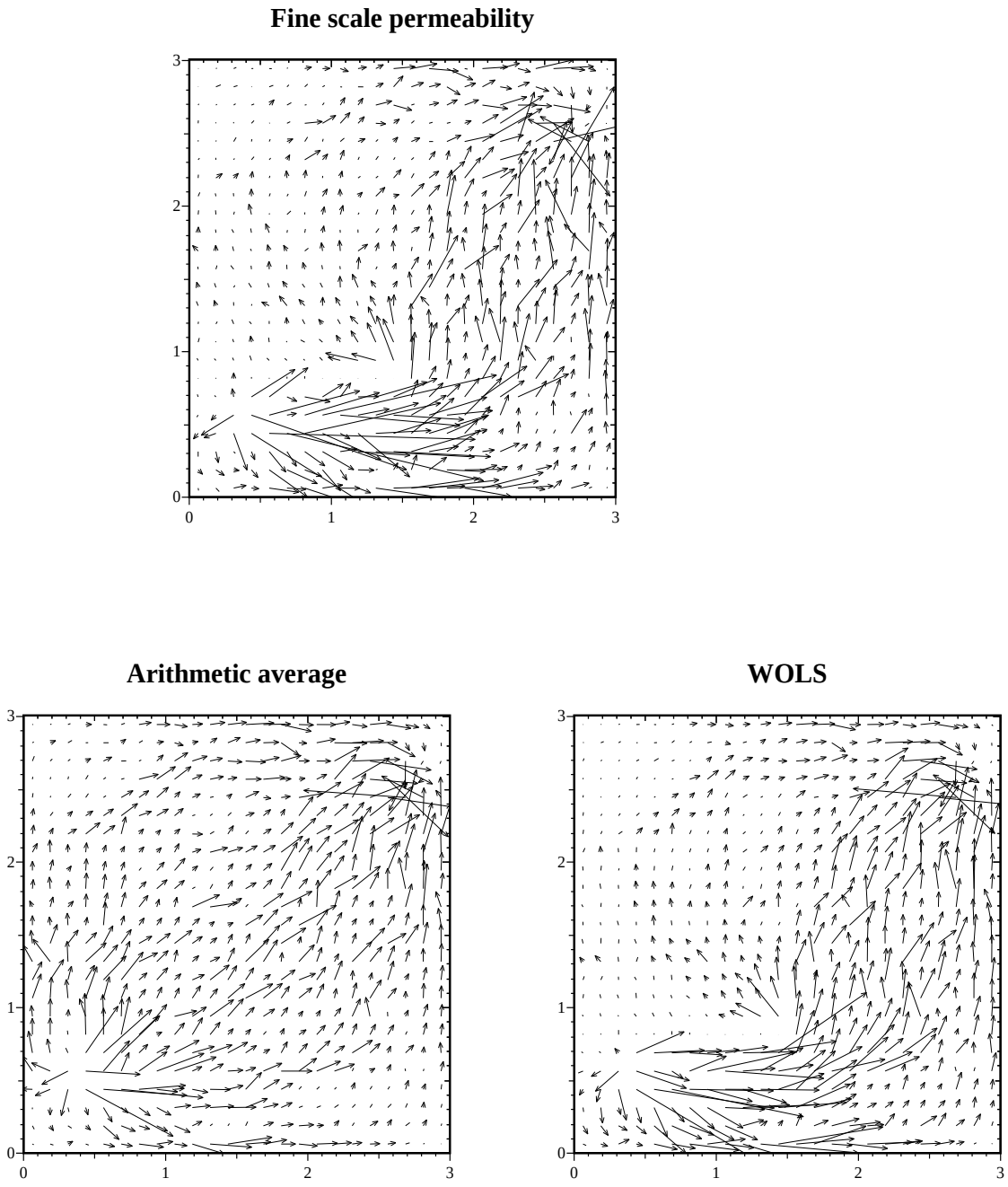

FIG. 5.11. *The figure shows the velocity fields for the problem studied in Case V c); upscaling from a* 64×64 *to a* 32×32 *mesh.*

[9] C. V. DEUTSCH, *Calculating effective absolute permeability in sandstone/shale sequences*, SPE Formation Evaluation, pp. 343–348, 1989.

[10] DIFFPACK HOME PAGE, *http://www.nobjects.com/diffpack*

[11] A. J. DESBARATS, *Numerical estimation of effective permeabilities in sand-shale formations*, Water Resour. Res., 23(2), pp. 273–286, 1987.

[12] L. J. DURLOFSKY, *Numerical calculation of equivalent grid block permeability tensors for het-*

erogeneous porous media, Water Resour. Res., vol. 27 no. 5, pp. 699–708, 1991.

[13] H. W. Engl, K. Kunisch and A. Neubauer, *Convergence rates for Tikhonov regularisation of non-linear ill-posed problems*, Inverse Problems 5, 1989, pp. 523–540.

[14] H. W. Engl, *Regularization methods for the stable solution of inverse problems*, Surv. Math. Ind.(1993) 3, pp. 71–143.

[15] R. Ewing, *Problems arising in the modeling of processes for hydrocarbon recovery*, The Mathematics of Reservoir Simulation, R. Ewing, Ed., SIAM, Philadelphia, 1983, pp. 3-34.

[16] R. Fletcher, *Practical methods of optimization*, 2nd edition, John Wiley & Sons, New York 1987.

[17] M. Griebel and S. Knapek, *Matrix-dependent multigrid-homogenization for diffusion problems*, Proceedings of the GAMM-Seminar "Modelling and Computation in Environmental Sciences", Stuttgart, 1995, Notes on Numerical Fluid Mechanics, Vieweg-Verlag, Braunschweig, 1996.

[18] J. J. Gomez-Hernandez and A. G. Journel, *Stochastic characterization of grid-block permeabilities: from point values to block tensors*, Proceedings of "2nd European Conference on the mathematics of oil recovery", D. Guérillot and O. Guillon (Editors), Éditions Technip, pp. 83–90, Paris 1990.

[19] L. Holden and O. Lia, *A Tensor Estimator for the Homogenization of Absolute Permeability*, Transport in Porous Media 8(1), 37-47, 1992.

[20] V. V. Jikov, S. M. Kozlov and O. A. Oleinik, *Homogenization of differential operators and integral functions*, Springer-Verlag, 1994.

[21] P. R. King, *The use of renormalization for calculating effective permeability*, Transport in porous media 4, 37-58, 1989.

[22] H. P. Langtangen, *Diffpack: Software for partial differential equations.* (In the proceedings of the 2nd Annual Object-Oriented Numerics Conference, Sunriver, Oregon), 1994.

[23] H. Omre, K. Sølna and H. Tjelmeland, *Simulation of random functions on large lattices*, Fourth International Geostatistical Congress, Proceedings, Troia, Portugal, September 13-18, 1992.

[24] D. W. Peaceman, *Fundamentals of Numerical Reservoir Simulation*, Elsevier, 1977.

[25] M. Dale, S. Ekrann and L. Holden, *Reservoir modelling; Effective properties*, in "Recent advances in improved oil recovery methods for north sea sandstone reservoirs", S. M. Skjæveland and J. Kleppe (eds.), Norwegian petroleum directorate, 1992.

[26] K. Suzuki, N. Kikuchi, *A homogenization method for shape and topology optimization*, Comput. Methods Appl. Mech. Eng. 93, No.3, 291-318, 1991.

[27] L. Tartar, *H-measures, a new approach for studying homogenisation, oscillations and concentration effects in partial differential equations*, Proc. R. Soc. Edinb., Sect. A 115, No.3/4, 193-230, 1990.

[28] K. Tyler, A. Henriques, A. Hektoen, L. Holden and A. MacDonald, *MOHERES - A collection of stochastic models for describing heterogeneities in clastic reservoirs*, Third International Conference on North Sea Oil and Gas Reservoirs, Proceedings, Trondheim November 30 - December 2, 1992.

[29] J. E. Warren and H. S. Price, *Flow in heterogeneous porous media*, Soc. Pet. Eng. J., pp. 14–28, 1961.